Автоматизированное проектирование опто-плазмонных схем, предназначенных для обработки информации классическими и квантовыми методами.

ПРОХОРОВ А.В.

Владимирский государственный университет им. А.Г. и Н.Г. Столетовых

I.
Полупроводниковые квантовые точки: оптически–управляемые центры обработки классических/квантовых состояний э.м. поля.

semiconductor quantum dots: discovery, triumph and new challenge

- ✓ Ekimov A. I., Onushchenko A. A., JETP Lett. 34, p.345, 1981;
- ✓ Ekimov A. I; USSR State Prize in Science and Engineering, 1975
- ✓ Ekimov A. I; R.W. Wood prize of the OSA, 2006

- ✓ QLED TV, Samsung Electronics, 2011

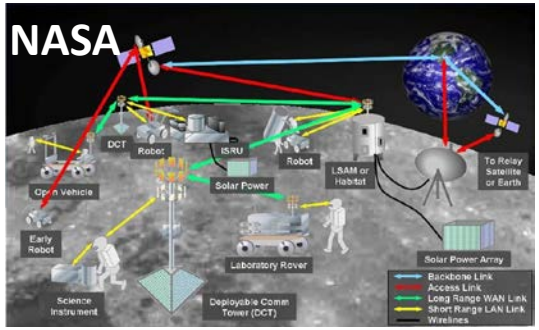

- ✓ Future Global Wireless THz/infrared Communications:
- ✓ D. Bimberg, VCSELs for 200+ Gbit/s data transmission
- ✓ S. Komiyama, THz and infrared photon detectors

QD. controllable properties of an artificial atom

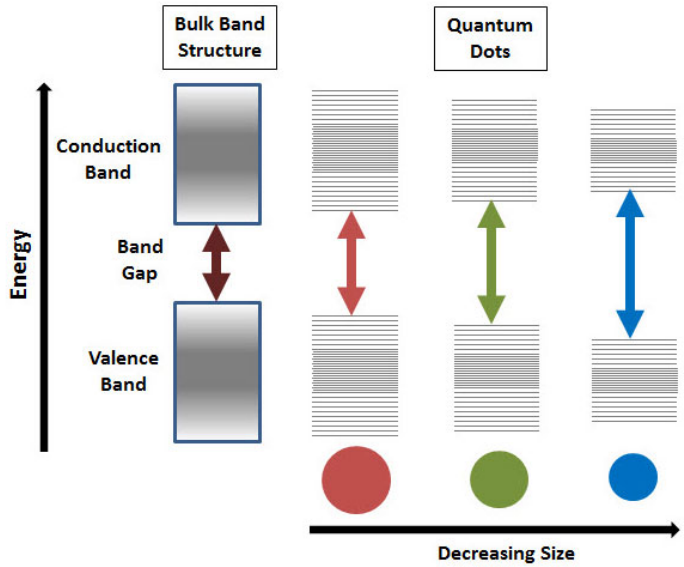

Interband transition frequency

$$\omega_{n'm} = \frac{1}{\hbar}\left(eE_g + \frac{\hbar^2}{2a^2}\left(\frac{\chi_{n'l'}^2}{m_e} + \frac{\chi_{nl}^2}{m_h}\right) - \frac{3.56e^2}{8\pi\varepsilon\varepsilon_0 a}\right)$$

Dipole moment of transition

$$p_0^2 = \frac{e^2}{6m_0{\omega_0}^2}\left(\frac{m_0}{m_e} - 1\right)\frac{\omega_0(\omega_0 + \Delta_0)}{\omega_0 + \frac{2\Delta_0}{3}}$$

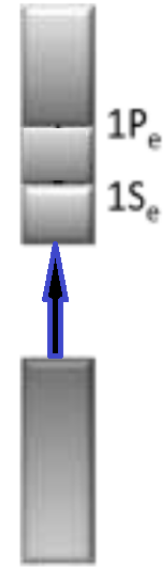

Intraband transition frequency

$$\omega_{m'n'} = \frac{1}{\hbar}\left(\frac{\hbar^2}{2m_e a^2}\left(\left|\chi_{m'k'}^2 - \chi_{n'l'}^2\right|\right)\right)$$

Dipole moment of transition

$$\mu_{if} = e\int_0^{2\pi}\int_o^{\pi}\int_0^{R} \psi_i^*(r,\theta,\varphi)\cdot r\cdot\psi_f(r,\theta,\varphi)\cdot r^2\sin\theta dr d\theta d\varphi$$

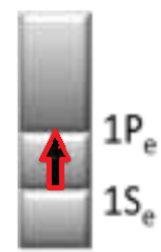

Bessel Function of the First Kind

$$\psi\ (r,\theta,\varphi) = \sqrt{\frac{2}{r}}\frac{1}{R}\frac{J_{l+1/2}(k_{nl}r)}{J_{l+3/2}(\chi_{nl})}Y_{lm}(\Theta,\phi),$$

spherical harmonics

properties optimization of QD-like particles

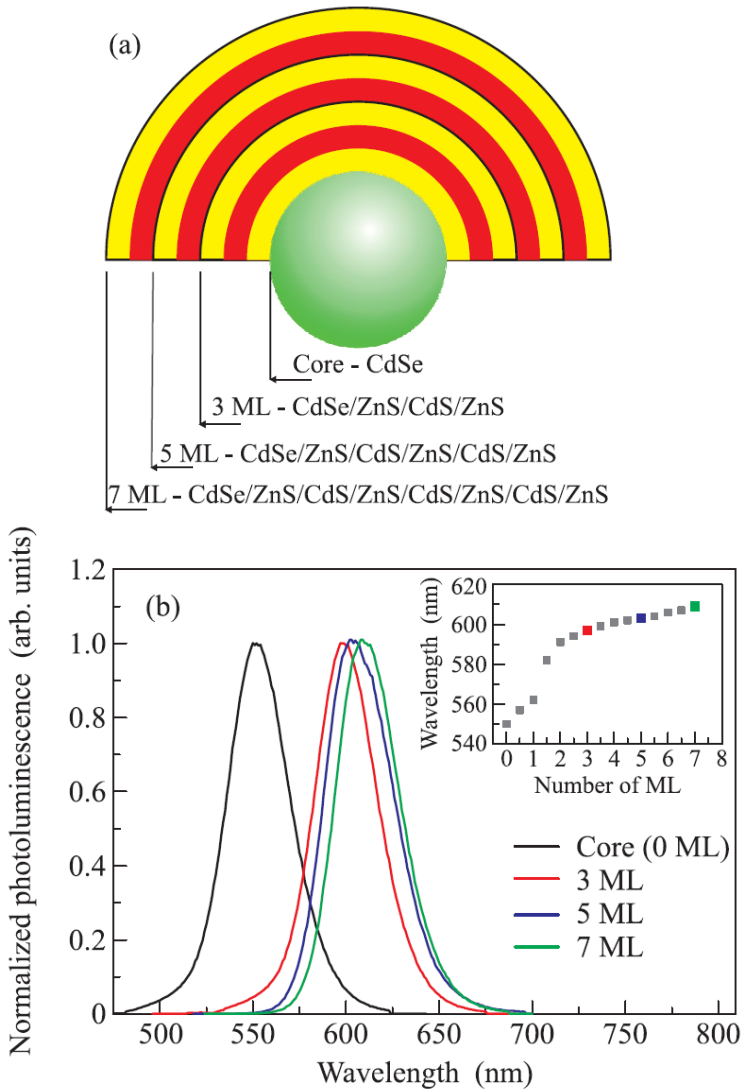

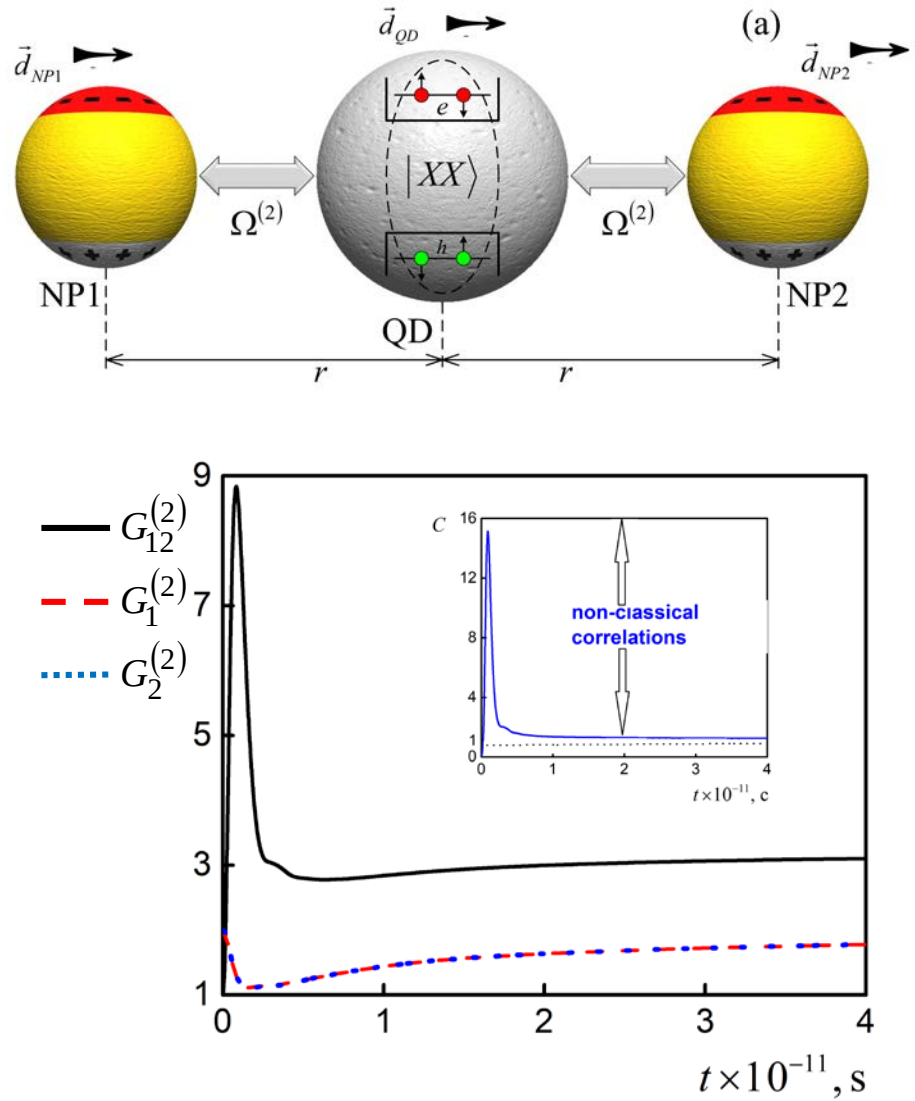

✓ **PL of core/n-shell QD**

Linkov P. et. al, JETP Lett., 109, p.108, 2019

✓ **Entangled states generation**

A. V. Prokhorov, et. al, Phys. Rev. B 97, 085431, 2018

Software

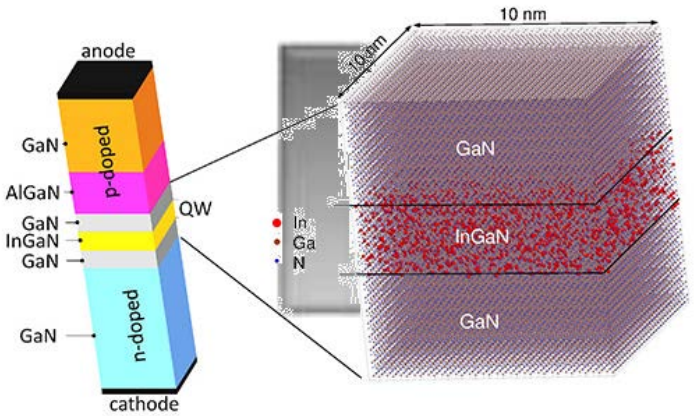

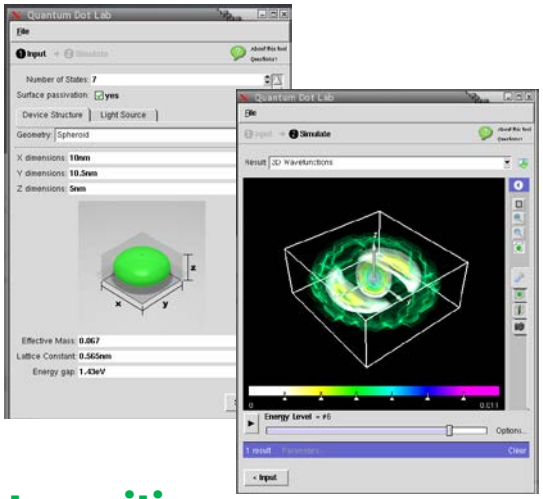

✓ **calculation of QD electronic properties**

Valence Force Field (VFF) from tiberCAD (IT)

✓ **QD Optical transitions,**

Quantum Dot Lab v. 1.x, Purdue University (UK)

http://test_plazm.expertpro.online/main/

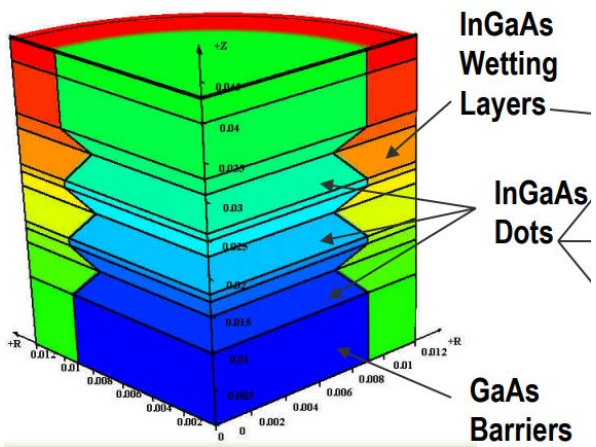

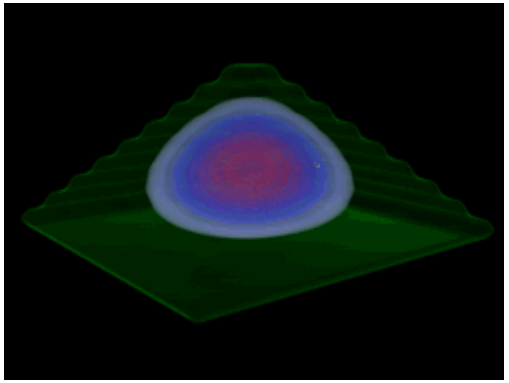

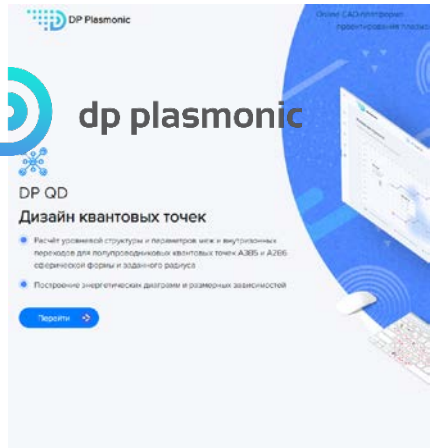

✓ **MOCVD simulation**

PROCOM from CrossLight (CA)

✓ **Full QD** analysis

NEMO 3-D (UK)

✓ **QD deign**

DP QD from dp Plasmonic (RU)

http://plazm.expertpro.online/main

II.
Фотонные/плазмонные схемы: управление распространением локализованных состояний э.м. поля.

optical waveguides

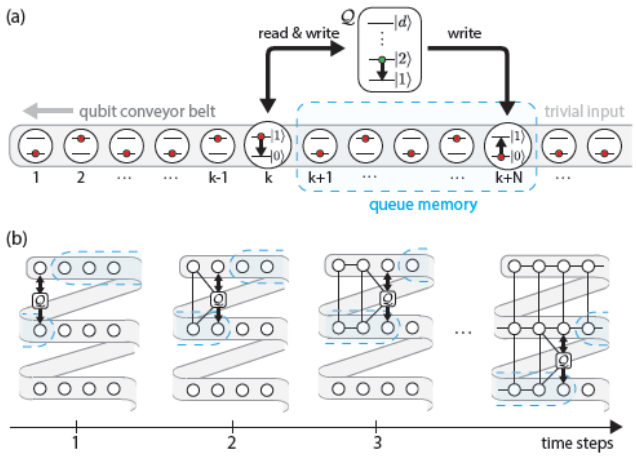

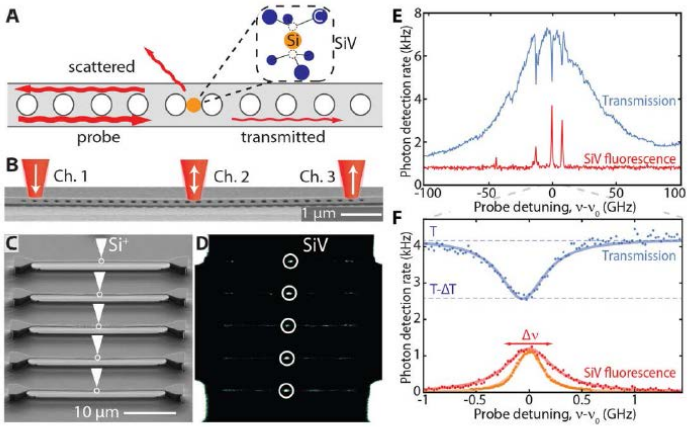

M. Lukin's group (Harvard University)

M. Lončar's group (Harvard University)

plasmonic waveguides

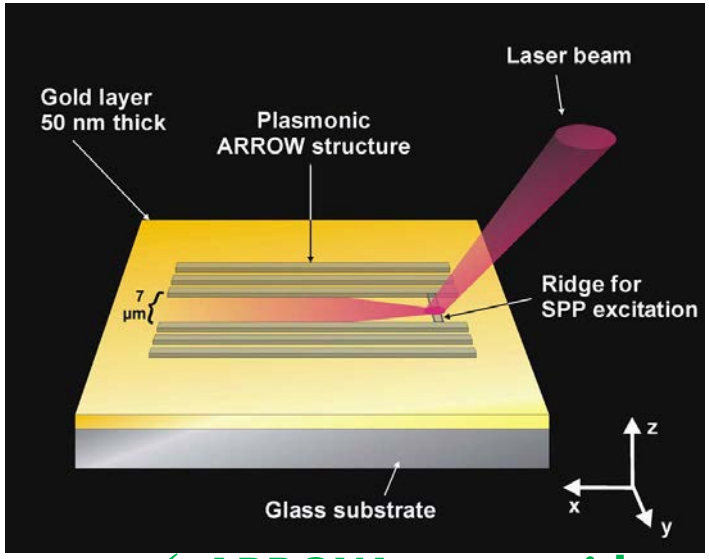

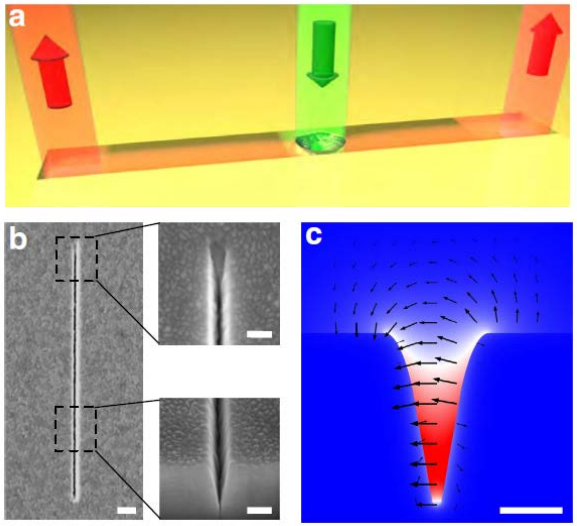

✓ **ARROW waveguides**

C. Reinhardt et. al, J. Opt. Soc. Am. B, 30, 2898, 2013

✓ **CPP-NV coupling**

Esteban Bermudez-Urena et. al, Nature communications, 6:7883, 2015

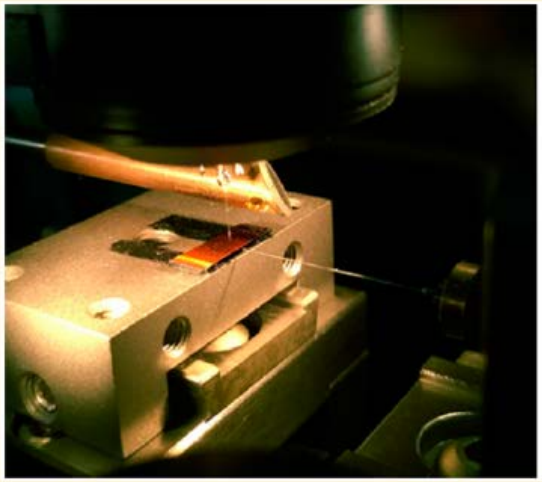

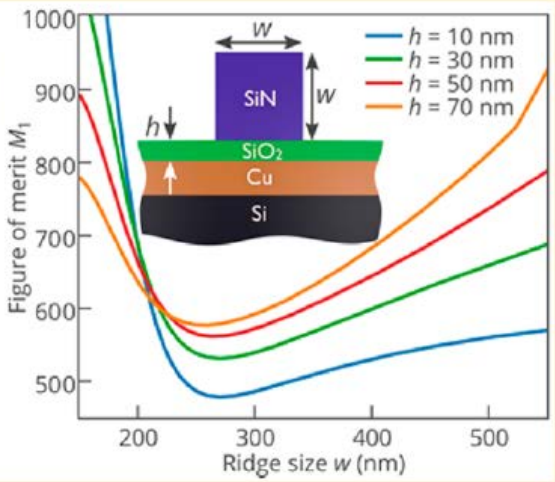

✓ **Copper Plasmonic Waveguides** **Valentyn S. Volkov et. al, Nano Lett., 16, 362, 2015**

graphene: perspective material for plasmonic waveguides

Kubo formula for total conductivity of graphene

$$\sigma_g(\omega,\mu_c,\tau,T) = \frac{-ie^2}{\omega+i/\tau}\int_0^\infty \epsilon\left(\frac{\partial f_d(\epsilon)}{\partial\epsilon}-\frac{\partial f_d(-\epsilon)}{\partial\epsilon}\right)d\epsilon - ie^2/\pi\hbar^2(\omega+i/\tau)\int_0^\infty \frac{f_d(\epsilon)-f_d(-\epsilon)}{(\omega+i/\tau)^2-4(\epsilon/\hbar)^2}d\epsilon$$

$$f_d(\epsilon) = 1/\left(e^{(\epsilon-\mu_c)/kT}+1\right)$$

Intraband (dominant under $|2\mu_c| > \hbar\omega$)

Interband (dominant under $|2\mu_c| < \hbar\omega$)

dielectric permittivity

$$\varepsilon_{gr} = 1 + i\frac{\sigma_g}{\omega\Delta_g\varepsilon_0}$$

effective index

$$n_{eff} = \sqrt{\varepsilon_d - \left(\frac{2\varepsilon_d\varepsilon_0 c}{\sigma_g}\right)^2}$$

GP wavelength

$$\lambda_{SPP} = \frac{\lambda_0}{n_{eff}}$$

propagation length

$$L_{SPP} = \frac{\lambda_0}{4\pi\mathrm{Im}\left(\frac{\lambda_0}{\lambda_{SPP}}\right)}$$

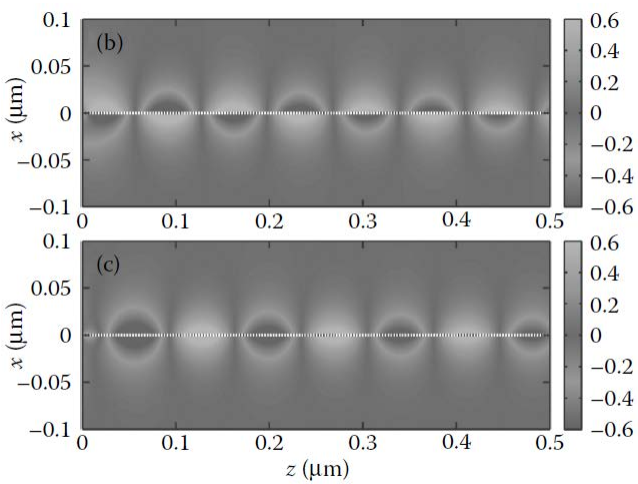

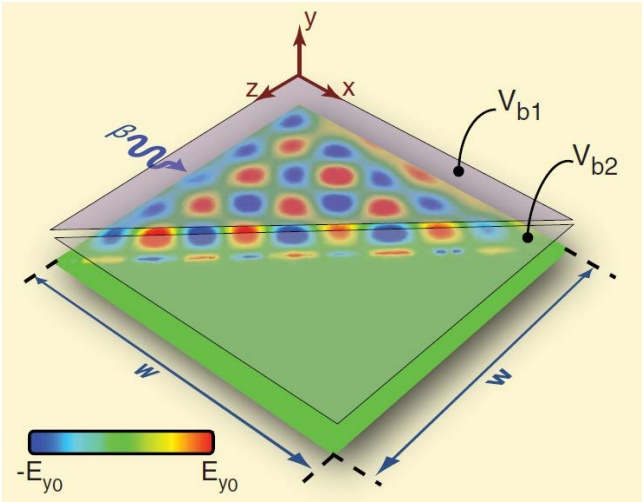

Wang, B., et. al, Phys. Rev. Lett. 109 (7):073901, 2012

Vakil, A. et. al, Science 332 (6035):1291, 2011

graphene waveguides

dispersion relation

$$-k_h\left(\pm e^{-k_h d} - 1\right) = 2ik_0 c\varepsilon_d\, \varepsilon_0/\sigma_g \equiv 2/\xi$$

weak coupling for $d > Re(\xi)$

strong coupling for $d < Re(\xi)$

two roots – two regimes

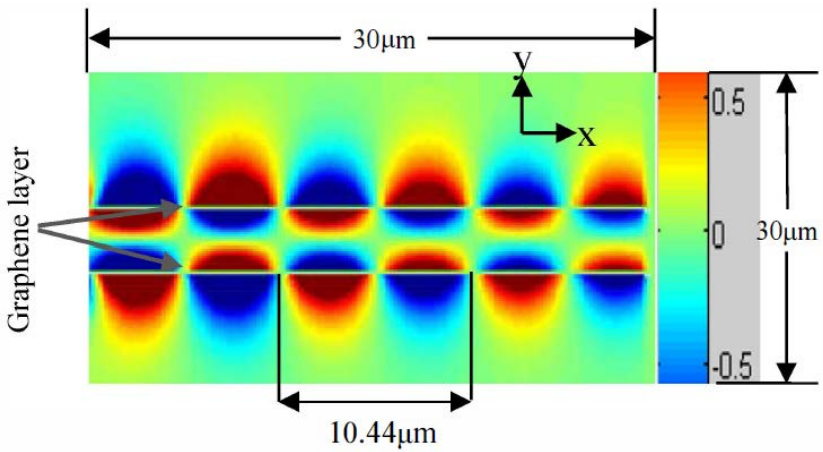

anti-symmetric mode

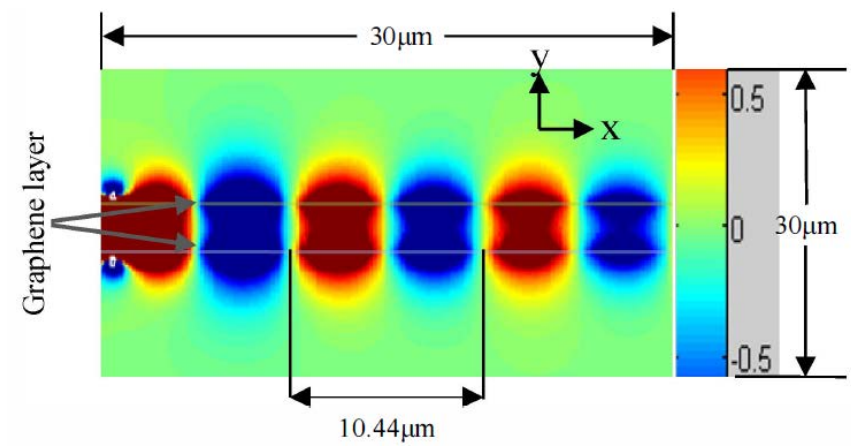

symmetric mode

Md. Masud Rana, et. al, ICEEICT, Bangladesh,2015

Curved waveguides

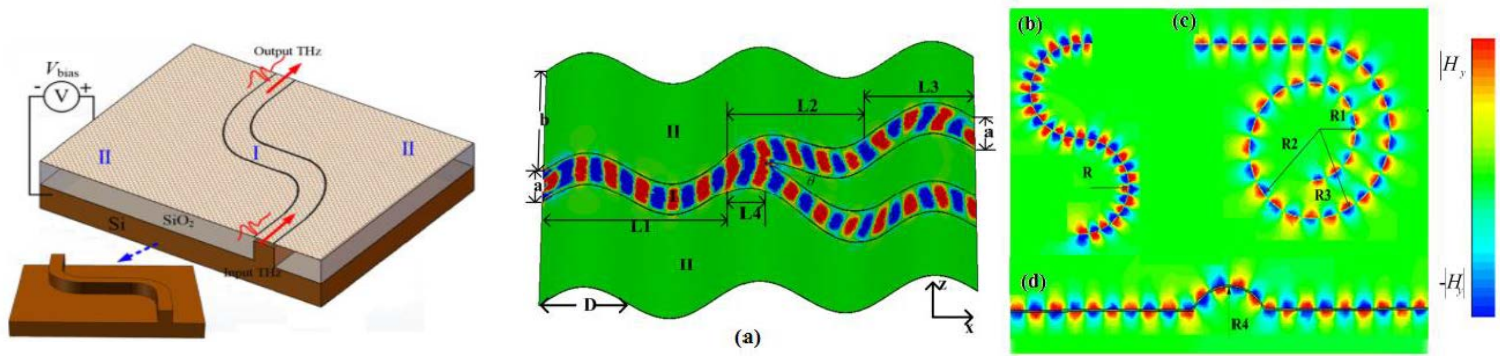

Lu, W.B., et al., Optics express,21(9): p. 10475, 2013

FDTD for full-wave electromagnetic simulation of SPP in graphene

calibration of algorithm

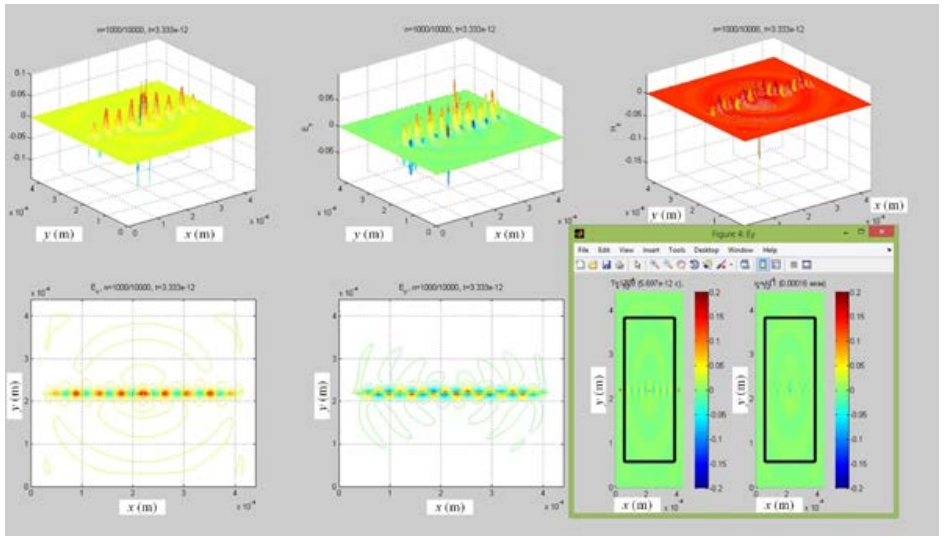

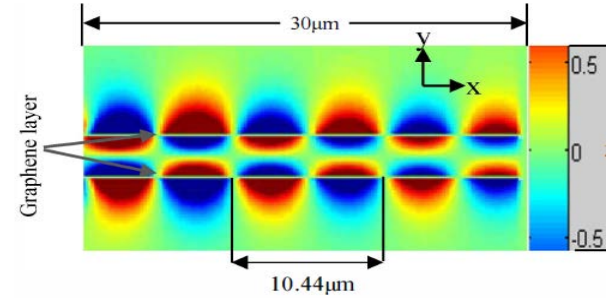

From Md. Masud Rana

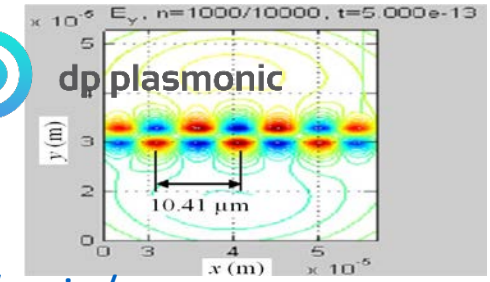

http://test_plazm.expertpro.online/main/ **by our Software**

graphene characterization results by our Software for IR range

GR

$\mu_c = 0.6$ eV

$\tau = 0.9$ ps,

$T = 300$ K,

$\Delta_g = 2$ nm

λ_0, μm	ε_d	$\frac{2\mu_c}{\hbar\omega_0}$	σ_1, S/m	σ_{intra}, S	σ_{inter}, S	single layer		double-layer sheet				
						λ_{SPP}, nm	L_{SPP}, μm	Re(ξ), nm	$n_{EF+}^{(R)}$	λ_{SPP+}, nm	L_C, nm	$\bar{L}_{SPP+}$, μm
4	1 (air)	3.88	$3.193 \cdot 10^7$	$3.5 \cdot 10^{-7} + 1.49 \cdot 10^{-4} i$	$2.51 \cdot 10^{-8} - 1.02 \cdot 10^{-5} i$	104.6	3.1	33	49	81.5	61	3.5
	2.103 (SiO_2)	3.88	$3.193 \cdot 10^7$	$3.5 \cdot 10^{-7} + 1.49 \cdot 10^{-4} i$	$2.51 \cdot 10^{-8} - 1.02 \cdot 10^{-5} i$	49.7	1.5	15.8	86.1	46.5	108.3	1.6
1.96	2.103 (SiO_2)	1.9	$3.193 \cdot 10^7$	$8.4 \cdot 10^{-8} + 7.3 \cdot 10^{-5} i$	$3.24 \cdot 10^{-8} - 2.26 \cdot 10^{-5} i$	8.86	0.3	2.82	221	8.86	$2.3 \cdot 10^6$	0.3
2.56	2.022	2.483	$3.193 \cdot 10^7$	$1.44 \cdot 10^{-7} + 9.54 \cdot 10^{-5} i$	$2.8 \cdot 10^{-8} - 1.65 \cdot 10^{-5} i$	18.8	0.7	6	136	18.8	2641	0.7
8.04	2.022	7.8	$3.193 \cdot 10^7$	$1.42 \cdot 10^{-6} + 3 \cdot 10^{-4} i$	$2.39 \cdot 10^{-8} - 4.98 \cdot 10^{-6} i$	224.2	3.8	71	59.3	135.5	74	3.7

III.
Функциональные элементы на основе локализованных состояний э.м. поля и квантоворазмерных хромофоров

Chromophore +graphene

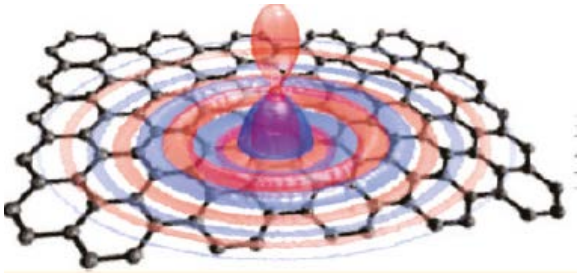

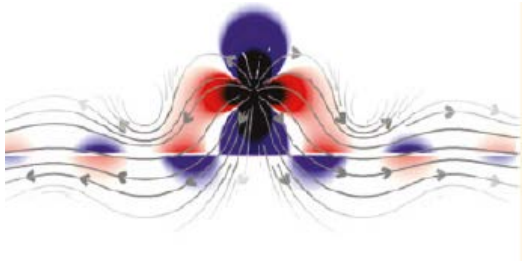

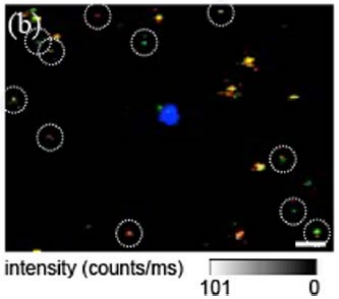

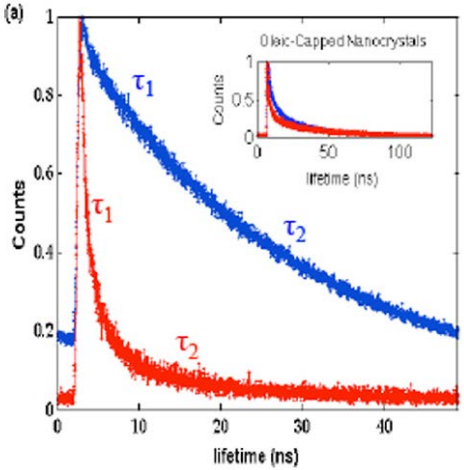

A Platform for Strong Light-Matter Interactions,

F. Javier García de Abajo et. al, Nano Lett., 11, 3370, (2011)

PL of QD near graphene,

Ajayi O. A., et. al, Appl. Phys. Lett. 95, 141103 (2009)

The basis for strong SPP-QD coupling

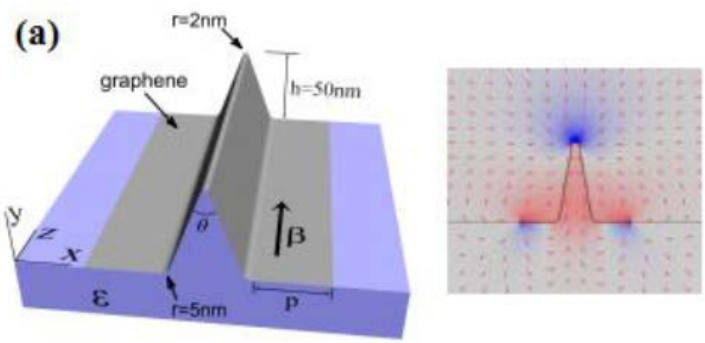

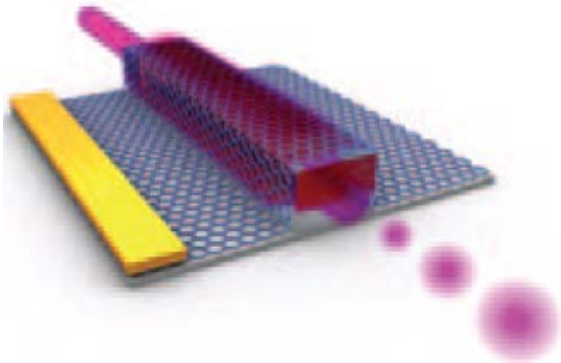

Liu, P., et al., Optics express, 21(26): p. 32432, 2013

Novoselov K.S., et. al, Nature photonics, 6, p. 749, 2012

GR waveguide integrated with stub-nanoresonator

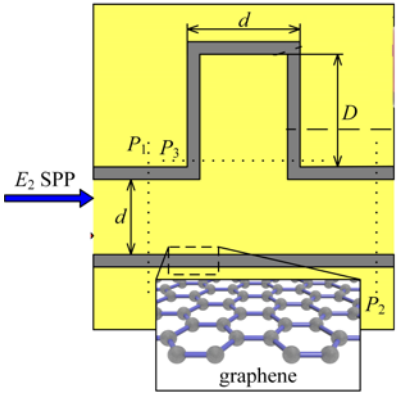

GR

$$\mu_c = 0.6 \text{ eV}$$

$$\tau = 0.9 \text{ ps}, T = 300 \text{ K}, \Delta_g = 2 \text{ nm}$$

waveguide

$$d = 20 \text{ nm} \quad D = 23.8 \text{ nm}$$

SPP parameters

$\lambda_2 = 8.04$ **μm for signal SPP**

$\lambda_{SPP} = 135.5$ **nm**

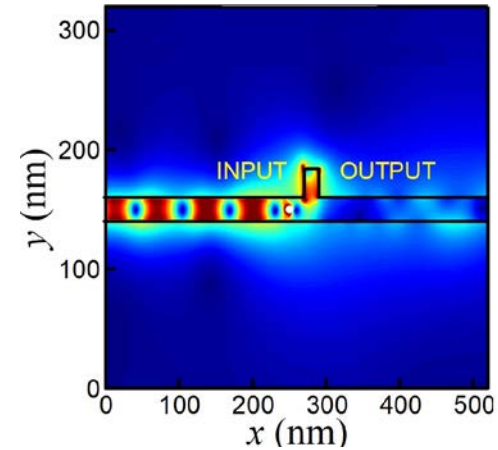

GR waveguide integrated with stub-nanoresonator loaded with CS QD

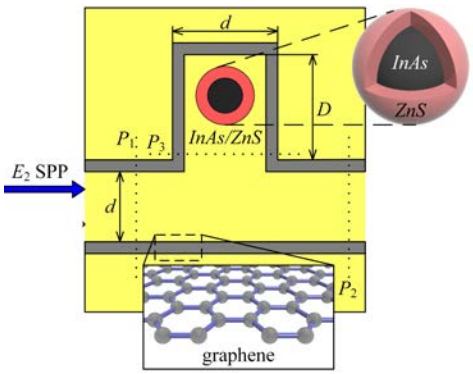

InAs/ZnS core-shell QD

core radius $a_{QD} = 9.9$ **nm**

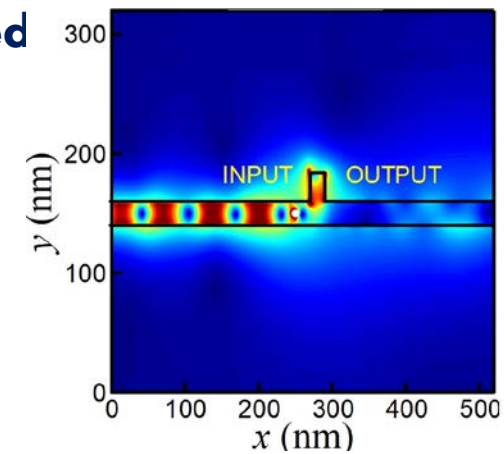

Ladder-type scheme of interaction in the stub with CS QD

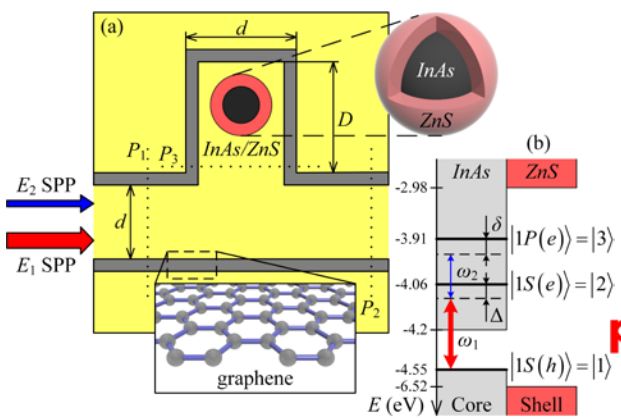

Pump SPP

$\lambda_1 = 2.56$ μm

$I_1/I_2 = 10$

Main effect

phase shift $\Delta\phi = \pi$ of signal SPP due to SPP-QD interaction

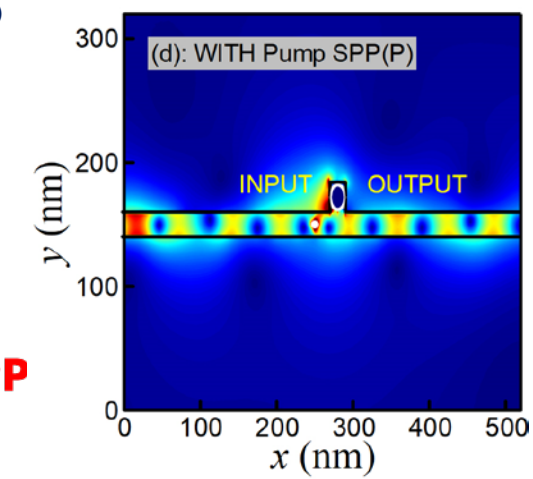

simulation

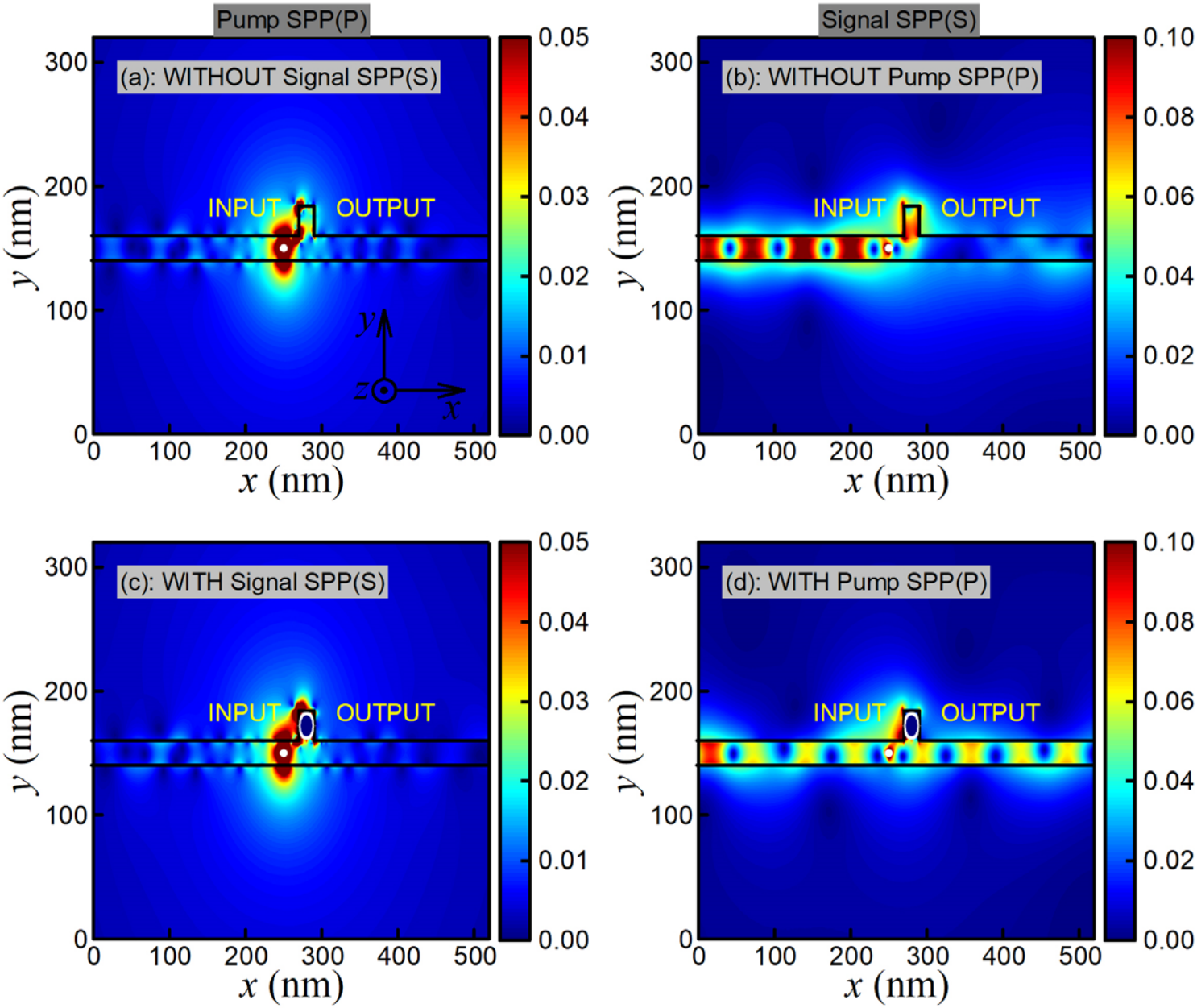

A. V. Prokhorov, et. al, arXiv: 1812.04487 [cond-mat.mes-hall]

tuning/bitrate

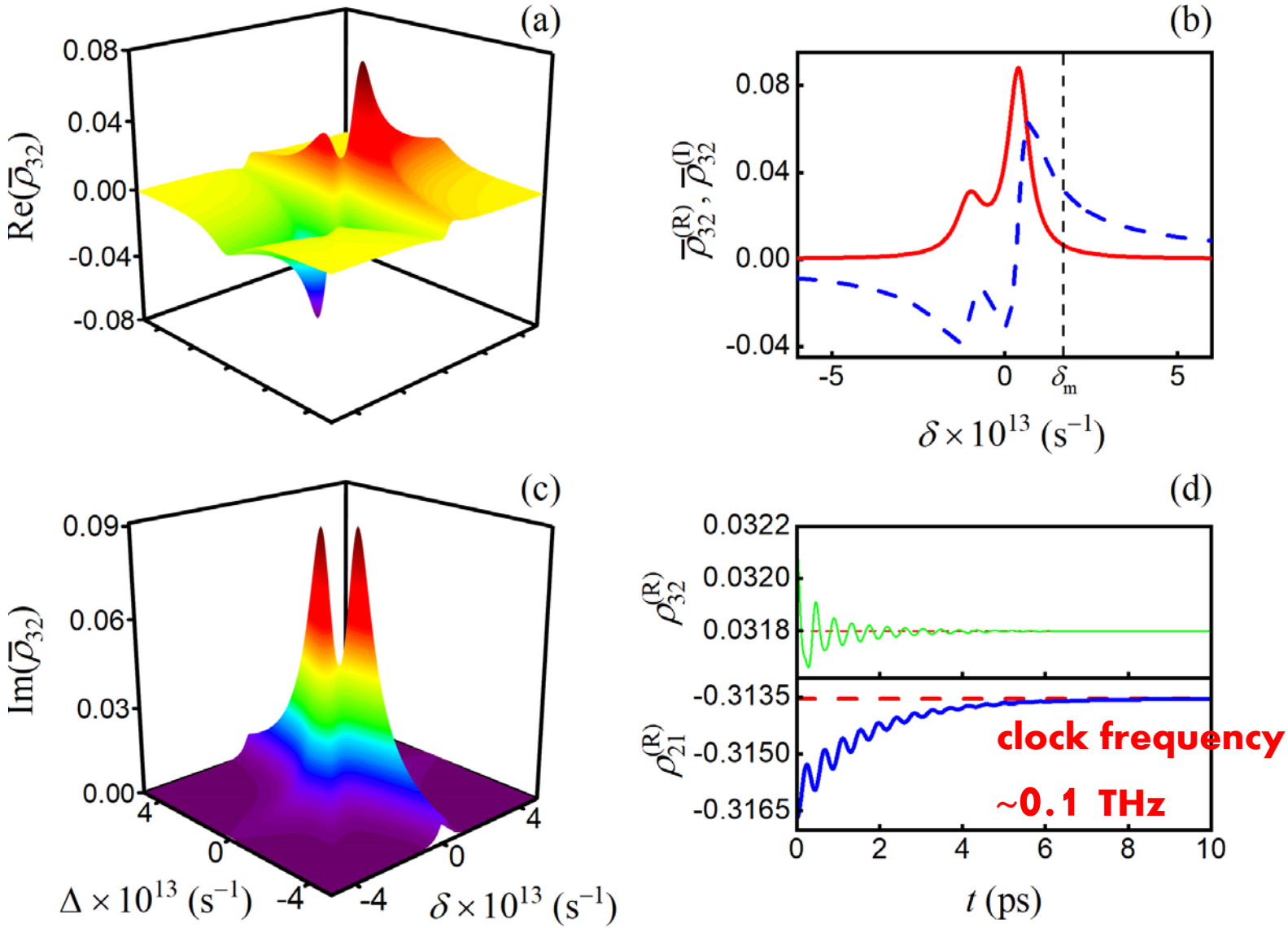

A. V. Prokhorov, et. al, arXiv: 1812.04487 [cond-mat.mes-hall]

fabrication

Materials and fabricating technology.

- **.Preparation of SiO_2 (Al_2O_3) substrate with recess corresponding to the further stub nanoresonator with height $D = 23.8$ nm.**
- **M1. Plasma enhanced chemical vapor deposition (PECVD) method for deposition of graphene on substrate. CH_4 Plasma Source. The thickness of graphene single layer is $\Delta_g = 2$ nm (chemical potential of graphene $\mu_c = 0.6$ eV, the time of electrons scattering is $\tau = 0.9$ ps).**
- **M2. Loading the InAs/ZnS core-shell QD (radius of core is 9.9 nm) into stub nanoresonator on the base of atomic force microscopy (AFM) nanomanipulation technique.**
- **M3. Pretreatment of graphene surface (oxidation or polymer coating). The polymer buffer layer between graphene and conventional gate dielectrics allows to achieve high carrier mobility.**
- **M4. The atomic layer deposition (ALD) method for deposition of dielectrics on graphene. The distance between graphene sheets is $d = 20$ nm**

For SiO_2 on graphene. Precursors $SiCl_4$ and H_2O or Silicon precursors.

For Al_2O_3 on graphene. Precursors $AlCl_3$-H_2O or trimethylaluminum (TMA; $Al(CH_3)_3$) and water (H_2O).

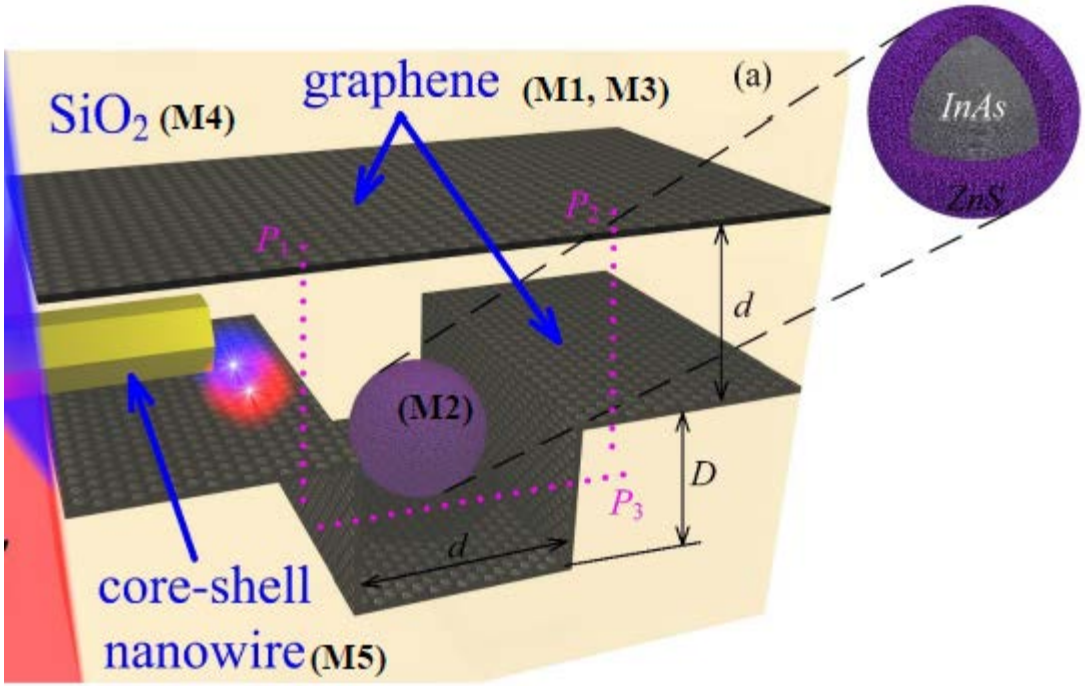

CINEMA

IV.
Наноразмерные квантовые гейты на основе гибридных систем.

Biexciton states as a base for photons entanglement

QD energy levels diagram

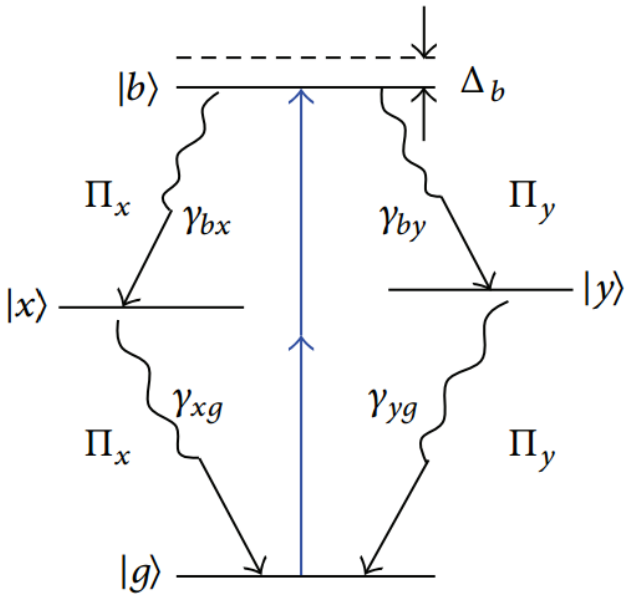

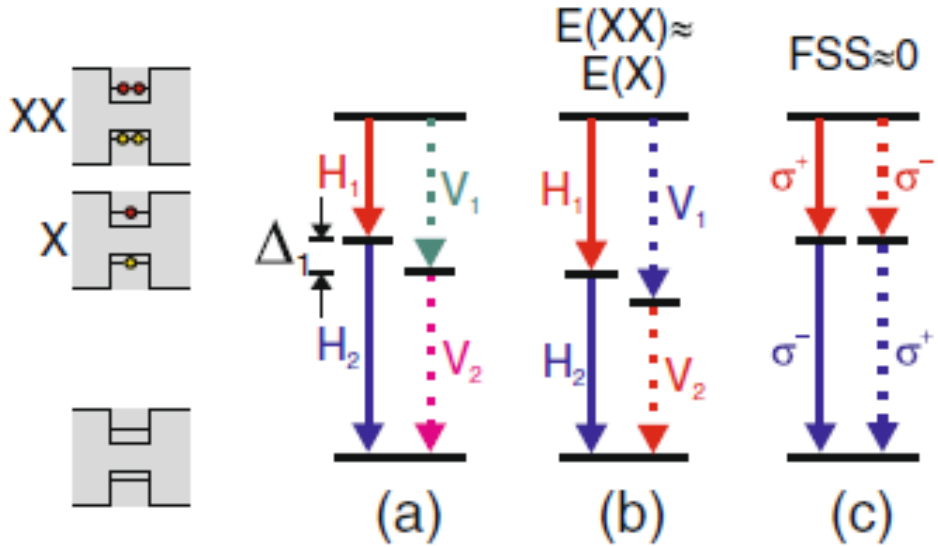

J. D. Plumhof et. al, Nanoscale Research Letters 2012, 7:336

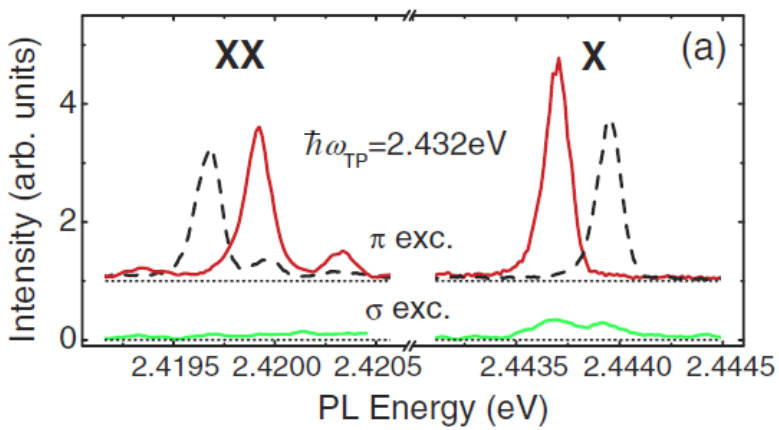

Akimov I.A.,PRL 96, 067401, 2006

a) $\Delta_1 \gg \gamma_{RAD}$: **classical cascade**

b) $\Delta_1 \gg \gamma_{RAD}$; $\omega_{Vi} = \omega_{Hj}$: **time-bin entanglement**

c) $\Delta_1 \ll \gamma_{RAD}$: **which–path quantum interference**

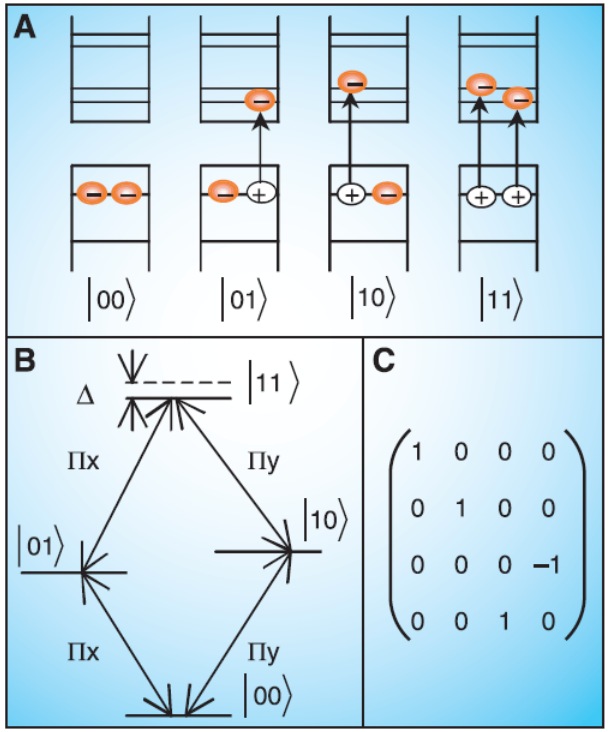

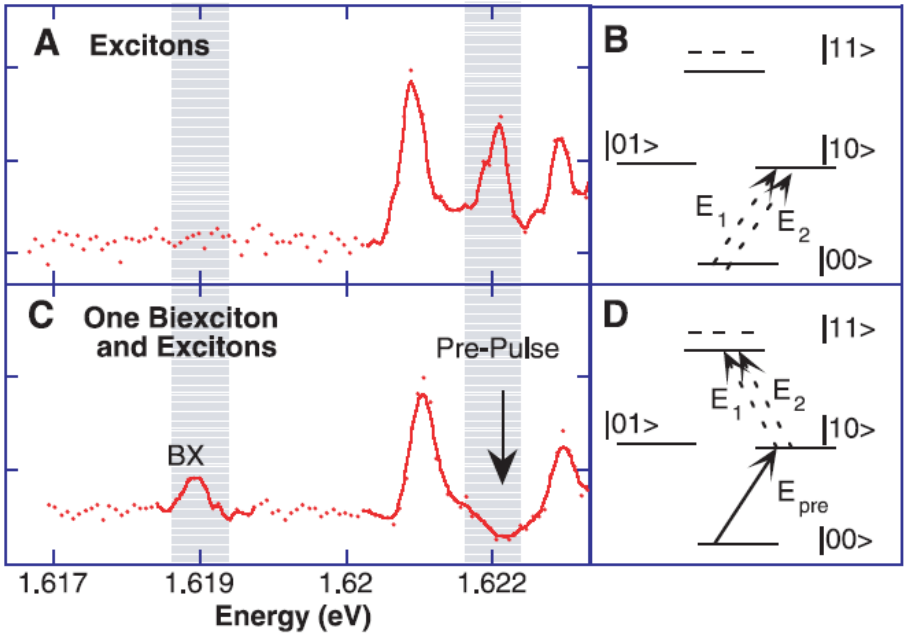

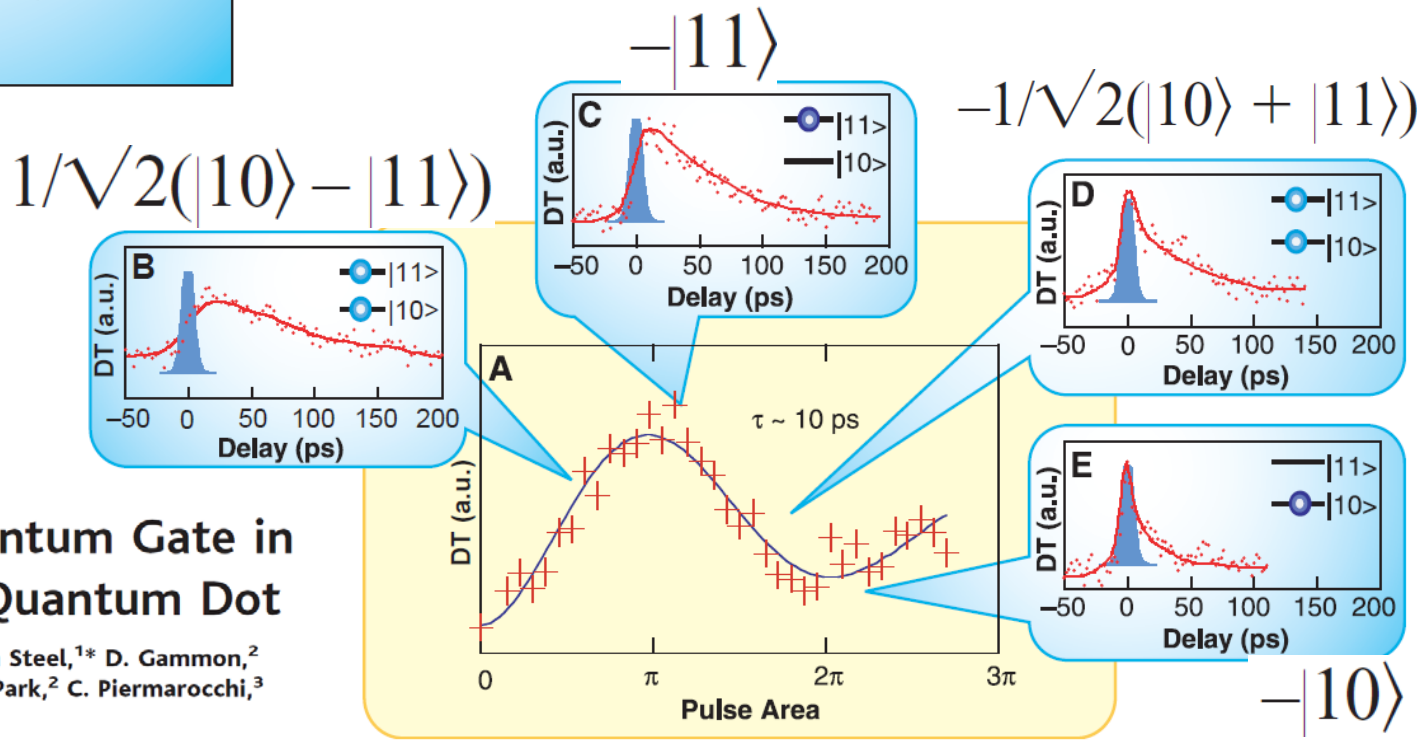

An All-Optical Quantum Gate in a Semiconductor Quantum Dot

Xiaoqin Li,[1] Yanwen Wu,[1] Duncan Steel,[1*] D. Gammon,[2] T. H. Stievater,[2] D. S. Katzer,[2] D. Park,[2] C. Piermarocchi,[3] L. J. Sham[4]

Biexciton states as a base for two-qubits gates

QD energy levels diagram

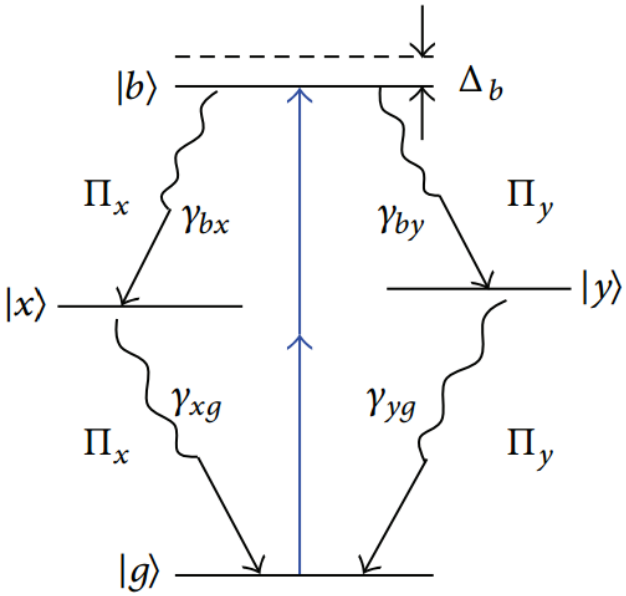

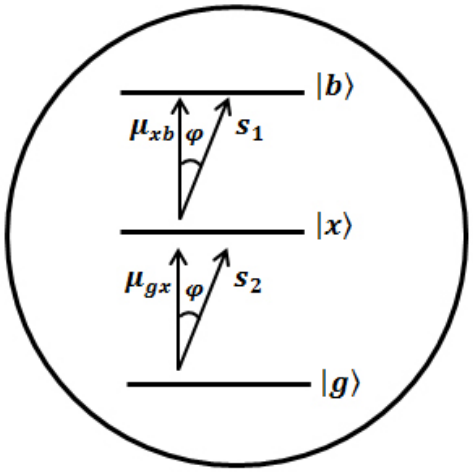

Left patch

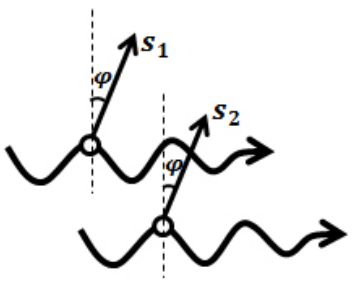

stimulation

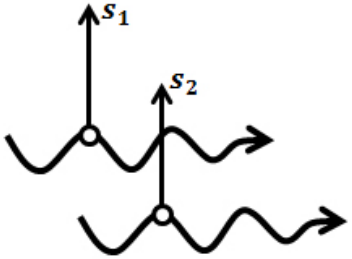

initialization

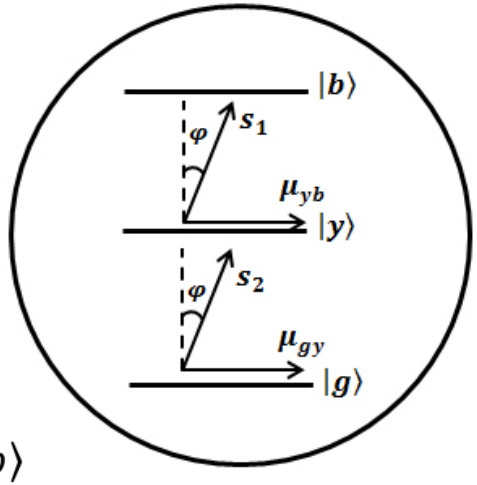

Right patch

the state of two-qubit register

$$\psi = \alpha|1\rangle_{c_1}|1\rangle_{c_2}|g\rangle + \beta|0\rangle_{c_1}|1\rangle_{c_2}|x\rangle + \gamma|1\rangle_{c_1}|0\rangle_{c_2}|y\rangle + \varepsilon|0\rangle_{c_1}|0\rangle_{c_2}|b\rangle$$

quantum dynamics

QD energy levels diagram

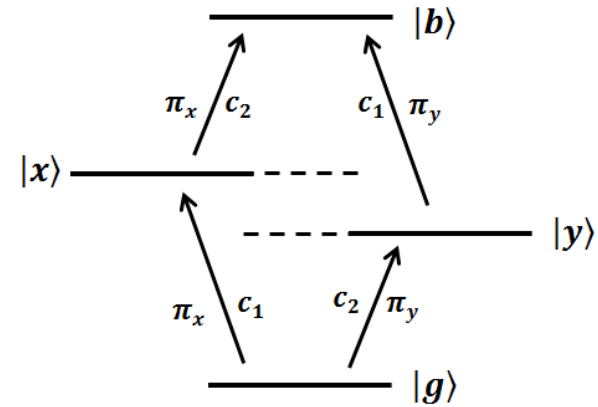

the Hamiltonian

$$H = -\hbar[\cos(\varphi)(g_1 c_1 S_x^+ + g_2 c_2 S_b^+ + g_1^* c_1^+ S_x + g_2^* c_2^+ S_b) + \\ +\sin(\varphi)(g'_2 c_2 S_y^+ + g'_1 c_1 S_b^+ + g'^*_2 c_2^+ S_y + g'^*_1 c_1^+ S_b)]$$

the state of two-qubit register

$$\psi = \alpha|1\rangle_{c_1}|1\rangle_{c_2}|g\rangle + \beta|0\rangle_{c_1}|1\rangle_{c_2}|x\rangle + \gamma|1\rangle_{c_1}|0\rangle_{c_2}|y\rangle + \varepsilon|0\rangle_{c_1}|0\rangle_{c_2}|b\rangle$$

$$\varphi = \pi, g = 10^{10}\ \mathrm{s}^{-1}$$

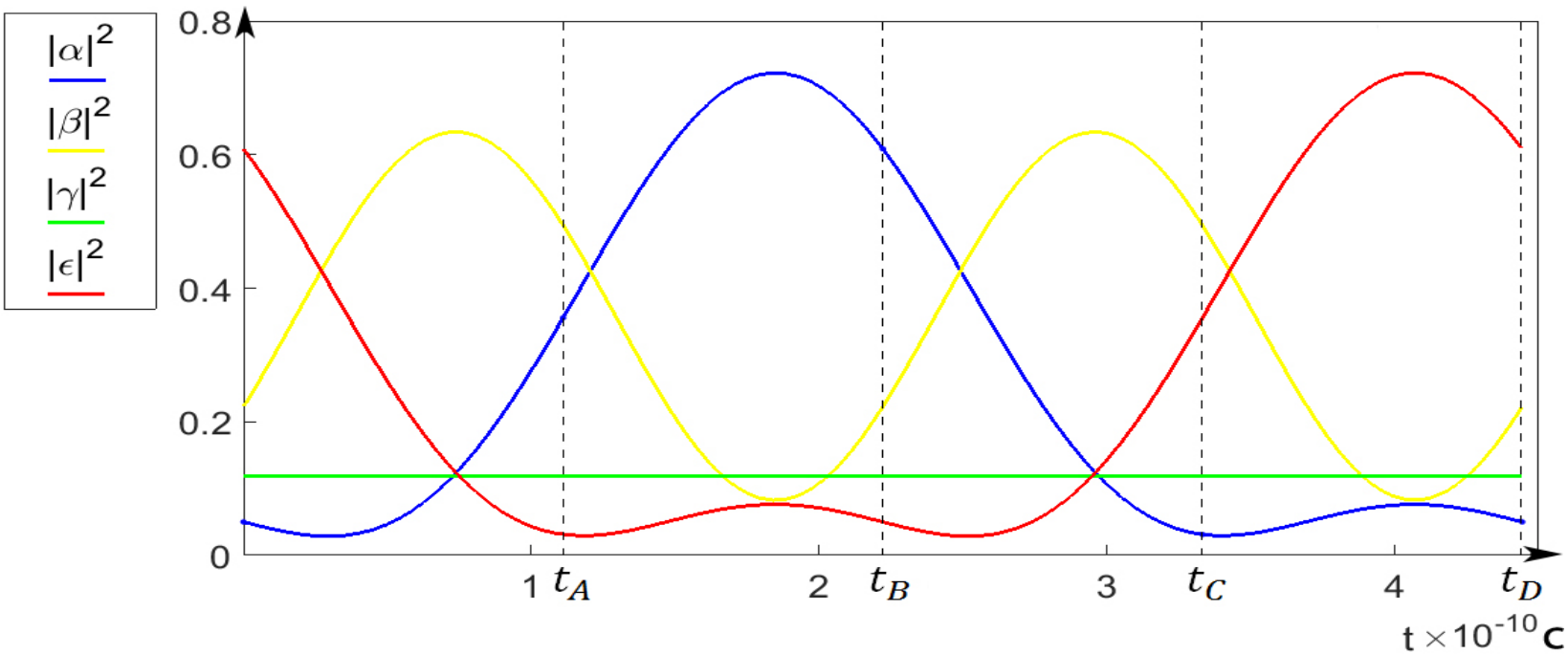

two-qubit gate

QD energy levels diagram

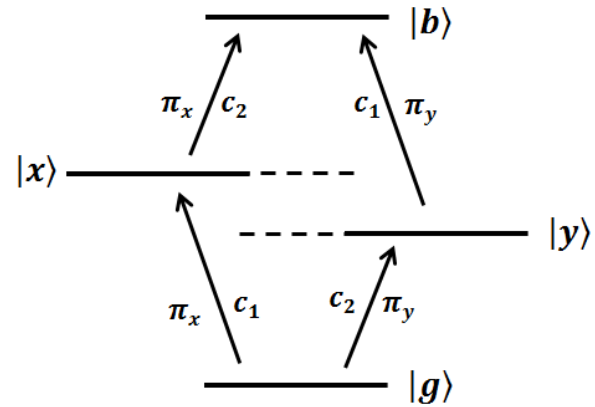

the Hamiltonian

$$H = -\hbar[\cos(\varphi)(g_1 c_1 S_x^+ + g_2 c_2 S_b^+ + g_1^* c_1^+ S_x + g_2^* c_2^+ S_b) + \\ +\sin(\varphi)(g'_2 c_2 S_y^+ + g'_1 c_1 S_b^+ + g'^*_2 c_2^+ S_y + g'^*_1 c_1^+ S_b)]$$

the state of two-qubit register

$$\psi = \alpha|1\rangle_{c_1}|1\rangle_{c_2}|g\rangle + \beta|0\rangle_{c_1}|1\rangle_{c_2}|x\rangle + \gamma|1\rangle_{c_1}|0\rangle_{c_2}|y\rangle + \varepsilon|0\rangle_{c_1}|0\rangle_{c_2}|b\rangle$$

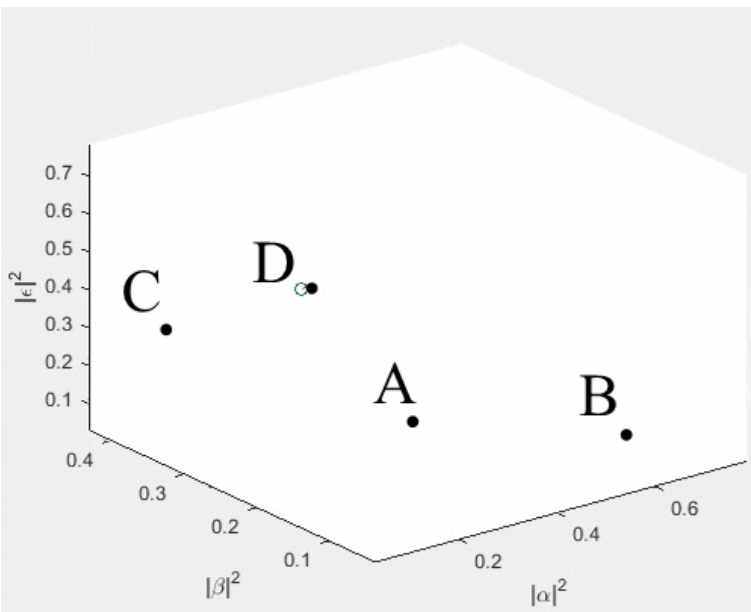

Quantum state transformation table ,

$g = 10^{10}\ \mathrm{s}^{-1}$, $t_B = 0{,}222$ ns

	in	out, t_A	out, t_B	out, t_C	out, t_D
$\lvert 1\rangle_{c_1}\lvert 1\rangle_{c_2}\lvert g\rangle$	α_0	$\frac{\alpha_0 - i\sqrt{2}\beta_0 - \varepsilon_0}{2}$	$-\varepsilon_0$	$\frac{\alpha_0 + i\sqrt{2}\beta_0 - \varepsilon_0}{2}$	α_0
$\lvert 0\rangle_{c_1}\lvert 1\rangle_{c_2}\lvert x\rangle$	β_0	$-\frac{i\alpha_0 + i\varepsilon_0}{\sqrt{2}}$	$-\beta_0$	$\frac{i\alpha_0 + i\varepsilon_0}{\sqrt{2}}$	β_0
$\lvert 1\rangle_{c_1}\lvert 0\rangle_{c_2}\lvert y\rangle$	γ_0	γ_0	γ_0	γ_0	γ_0
$\lvert 0\rangle_{c_1}\lvert 0\rangle_{c_2}\lvert b\rangle$	ε_0	$\frac{-\alpha_0 - i\sqrt{2}\beta_0 + \varepsilon_0}{2}$	$-\alpha_0$	$\frac{-\alpha_0 + i\sqrt{2}\beta_0 + \varepsilon_0}{2}$	ε_0

quantum dynamics

QD energy levels diagram

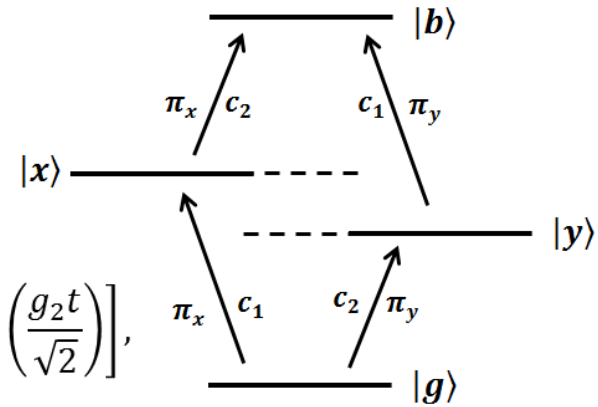

$$\varphi = \frac{\pi}{4},$$

$$\dot{\alpha} = \cos\left(\frac{g_1 t}{\sqrt{2}}\right)\left[\alpha_0 \cos\left(\frac{g_2 t}{\sqrt{2}}\right) + i\gamma_0 \sin\left(\frac{g_2 t}{\sqrt{2}}\right)\right] + \sin\left(\frac{g_1 t}{\sqrt{2}}\right)\left[i\beta_0 \cos\left(\frac{g_2 t}{\sqrt{2}}\right) - \varepsilon_0 \sin\left(\frac{g_2 t}{\sqrt{2}}\right)\right],$$

$\dot{\beta}$=...

$$K = {g_1}^2 + {g_2}^2;\ \theta = \sqrt{{g_1}^2 + {g_2}^2}\,t = \frac{\pi}{2}.$$

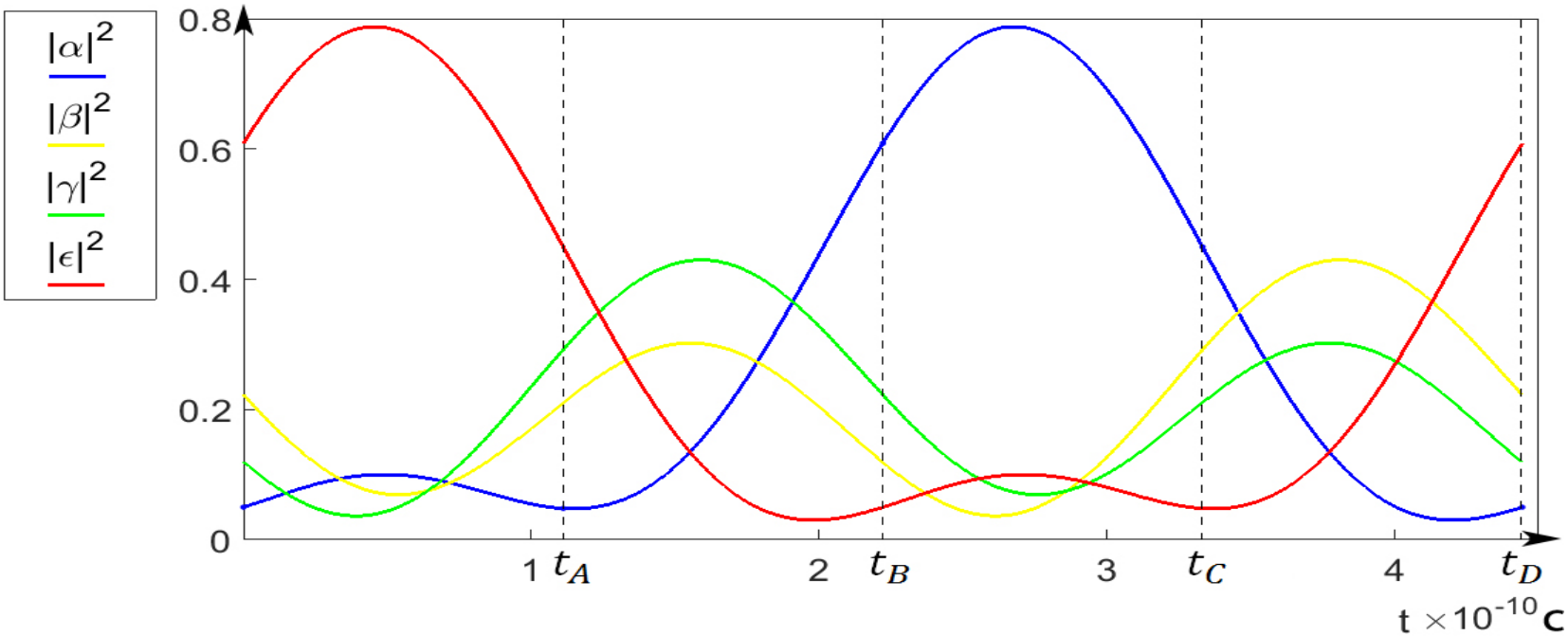

two-qubit gate

QD energy levels diagram

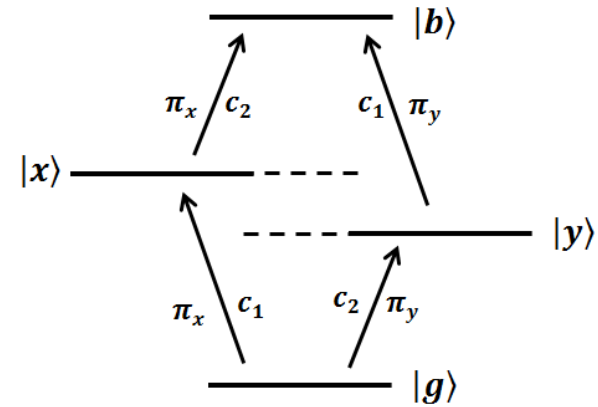

the state of two-qubit register

$$\psi = \alpha|1\rangle_{c_1}|1\rangle_{c_2}|g\rangle + \beta|0\rangle_{c_1}|1\rangle_{c_2}|x\rangle + \gamma|1\rangle_{c_1}|0\rangle_{c_2}|y\rangle + \varepsilon|0\rangle_{c_1}|0\rangle_{c_2}|b\rangle$$

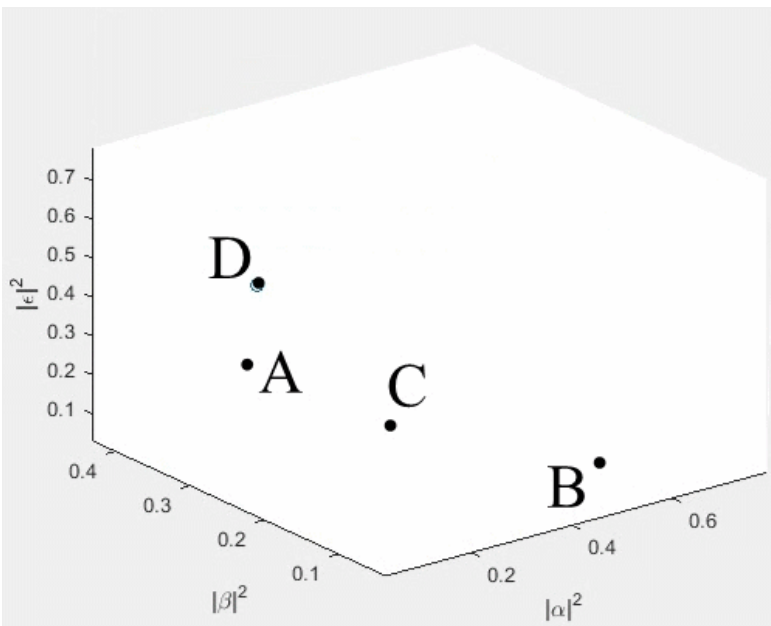

quantum state transformation table ,

$g = 10^{10}\ \mathrm{s}^{-1}$, $t_A = 0{,}111$ ns, $t_C = 0{,}333$ ns

	in	out, t_A	out, t_B	out, t_C	out, t_D
$\|1\rangle_{c_1}\|1\rangle_{c_2}\|g\rangle$	α_0	$\frac{\alpha_0 + i\beta_0 + i\gamma_0 - \varepsilon_0}{2}$	$-\varepsilon_0$	$\frac{\alpha_0 - i\beta_0 - i\gamma_0 - \varepsilon_0}{2}$	α_0
$\|0\rangle_{c_1}\|1\rangle_{c_2}\|x\rangle$	β_0	$\frac{i\alpha_0 + \beta_0 - \gamma_0 + i\varepsilon_0}{2}$	$-\gamma_0$	$\frac{-i\alpha_0 + \beta_0 - \gamma_0 - i\varepsilon_0}{2}$	β_0
$\|1\rangle_{c_1}\|0\rangle_{c_2}\|y\rangle$	γ_0	$\frac{i\alpha_0 - \beta_0 + \gamma_0 + i\varepsilon_0}{2}$	$-\beta_0$	$\frac{-i\alpha_0 - \beta_0 + \gamma_0 - i\varepsilon_0}{2}$	γ_0
$\|0\rangle_{c_1}\|0\rangle_{c_2}\|b\rangle$	ε_0	$\frac{-\alpha_0 + i\beta_0 + i\gamma_0 + \varepsilon_0}{2}$	$-\alpha_0$	$\frac{-\alpha_0 - i\beta_0 - i\gamma_0 + \varepsilon_0}{2}$	ε_0

Opto-plasmonic circuits

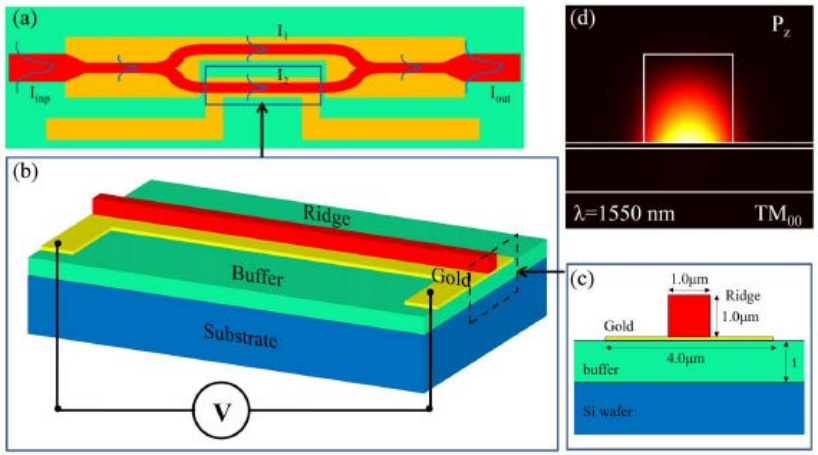

Sergey I. Bozhevolnyi (Denmark)

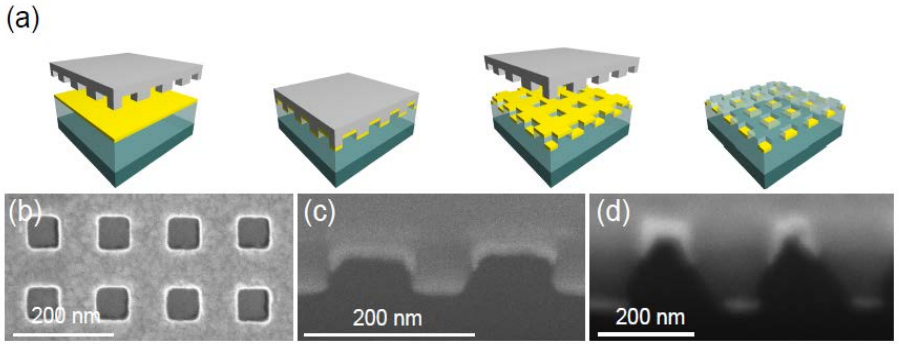

Valentin Flauraud, Ecole Polytechnique Fédérale de Lausanne, Switzerland

Plasmonic nm-process

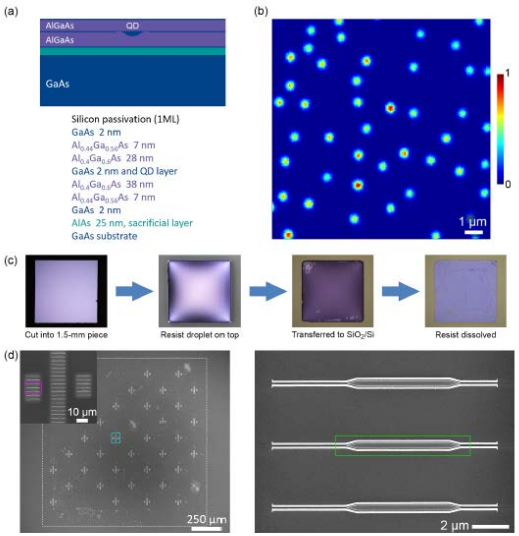

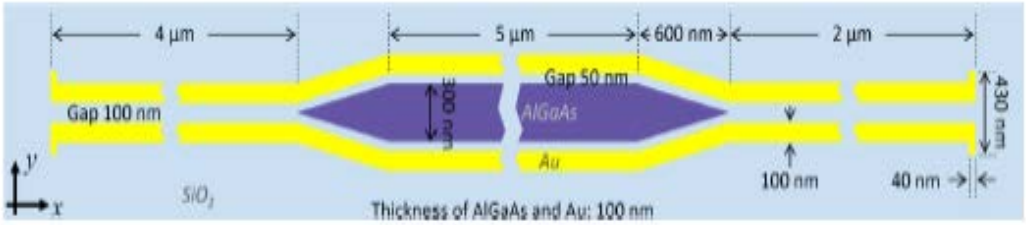

Markus Lippitz, Bayreuth, Germany